

COMPARISON OF RESULTS FROM PHYSICAL AND NUMERICAL MODELLING OF FLOW AND DISPERSION IN AND AROUND THE PICADA FIELD SITE STREET CANYON CONFIGURATION

Photios Barmpas¹, Nicolas Moussiopoulos¹ and Michael Schatzmann²

¹Aristotle University, Laboratory of Heat Transfer and Environmental Engineering (AUT
LHTEE), Thessaloniki, Greece

²University of Hamburg, Centre for Marine and Atmospheric Research, Meteorological
Institute (MIHU), Hamburg, Germany

INTRODUCTION

The aim of the PICADA project as *Photocatalytic Innovative Coverings Applications for Depollution Assessment* is to elaborate a range of façade coatings including a component that has self-cleaning and depolluting properties (*Moussiopoulos et al. 2005*). Motivated by the potential presented within the frame of the EU ATREUS project as *Advanced Tools for Rational Energy Use toward Sustainability* which emphasises on microclimatic issues in urban applications, a wind tunnel campaign was undertaken in order to investigate the flow and dispersion in and around the experimental street canyon configuration used during the PICADA field campaign (*Barmpas et al. 2005*). Additionally, a numerical study with the microscale model MIMO was conducted in order to compare numerical results with wind tunnel measurements and validate MIMO.

The model set up of the field site consisted of three consecutive street canyons of aspect ratio 0.4, with a line source of emissions having been placed along the entire length of the second consecutive street canyon of the model. Systematic velocity and concentration measurements were made, in order to investigate the effect of the approaching flow on the developing flow field and the corresponding pollution dispersion pattern under different approach flow directions. Flow visualisation experiments using laser light sheet techniques were carried out in an effort to better understand (1) the dynamics of the pollutant dispersion inside this specific street canyon and (2) the effect of different approach flow directions on both the vertical and horizontal transport of pollutants inside and outside the street canyon. Results from model simulations were extracted at the same locations of the wind tunnel measurements.

METHODOLOGY

Due to various technical considerations and since we were primarily interested on investigating the flow and dispersion fields inside the street canyon, a rather large scale of 1/50 had to be chosen (Figures 1a, 1b). For this scale, the blockage ratio was found to be 2.68%, which is well below the limits suggested by the guideline VDI 3783/Part 12. As a result, we were able to model only the lower part of the boundary layer up to a height $Z = 25\text{m}$. Due to lack of corresponding in-situ measurements, the modelled approach flow characteristics were assumed in accordance with the guideline VDI 3783/Part 12 for approach wind flows over rough surfaces. For that reason, appropriate vortex generators and roughness elements (20mm high LegoTM blocks) were used in the flow development section (Figure 1a). Both uniformity and reproducibility tests of the approach flow boundary layer were carried out at a distance 7H upstream of the model (Figure 2).

Additionally, a set of 3D numerical simulations for the full scale field site model were performed with the microscale model MIMO (*Ehrhard et al., 2000; Kunz, 2001*), for the case of the approach flow wind direction being perpendicular to the street canyon axis. The

computational domain and the mesh that were used along with the local grid refinement near the walls are shown in figure 3. At the inlet of the computational domain, an approach flow velocity profile measured in the wind tunnel at a distance of 3.5H upstream of the field site model with a corresponding estimated roughness height $z_o = 0.4$ was used as an inflow boundary condition. Moreover, at the outlet of the domain an open condition was assumed, while at the lateral and top boundaries of the domain symmetry conditions were applied. Turbulence was modelled with the standard $\kappa\text{-}\epsilon$ two equations model, using the standard wall functions.

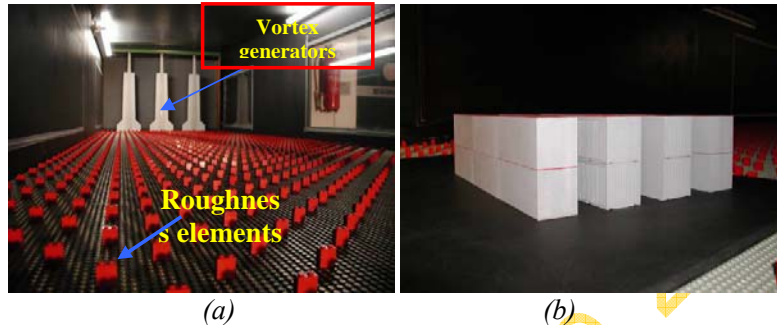


Fig. 1; Model in the scale 1/50: (a) Roughness elements and vortex generators (b) idealised urban roughness.

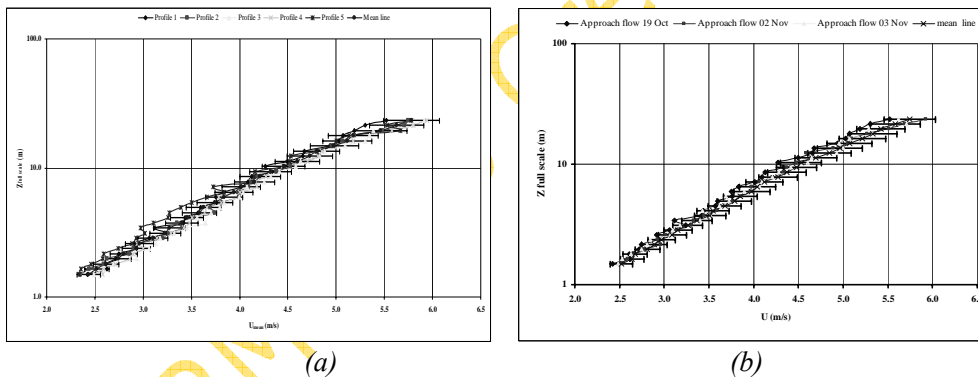


Fig. 2; (a) Uniformity tests, (b) Reproducibility test.

RESULTS AND DISCUSSION

For wind directions perpendicular (90°) to the street canyon axis, vertical U-W velocity components were measured upstream and downstream from the container array as well as above and inside the 2nd consecutive street canyon. For this case, horizontal U-V velocity components were also measured at three different height levels inside the 2nd consecutive street canyon namely at $Z = 0.3H$, $Z = 0.5H$ and at the roof top level.

Additional horizontal U-V measurements were made at height $Z = 0.5H$ upstream, downstream and at the side of the model. Furthermore, for this case detailed concentration measurements at various locations in and around the modelled street canyon configuration were made. Dimensionless concentration and normalised u- velocity component numerical results were extracted at the same locations as the wind tunnel measurements and comparison between the two was made in order to evaluate the performance of MIMO. Comparison between numerical results and wind tunnel measurements at various locations shows good agreement between the two (Figures 4-6).

Both the wind tunnel measurements and the numerical results indicate that when the wind direction is perpendicular to the street canyon axis, pollutants concentrate mainly at the middle cross section of the street canyon, with the exchange of air being dominated by vertical transport.

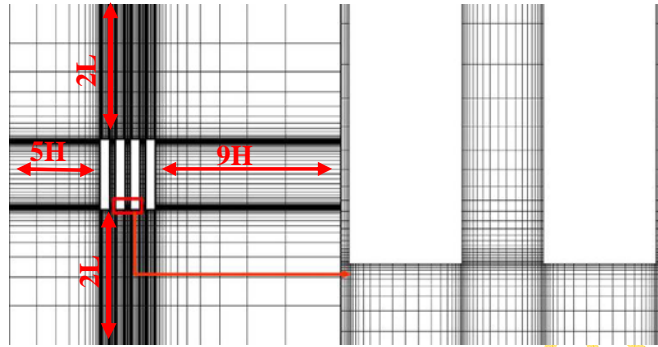


Fig. 3; Computational domain and mesh used for the 3D numerical simulation.

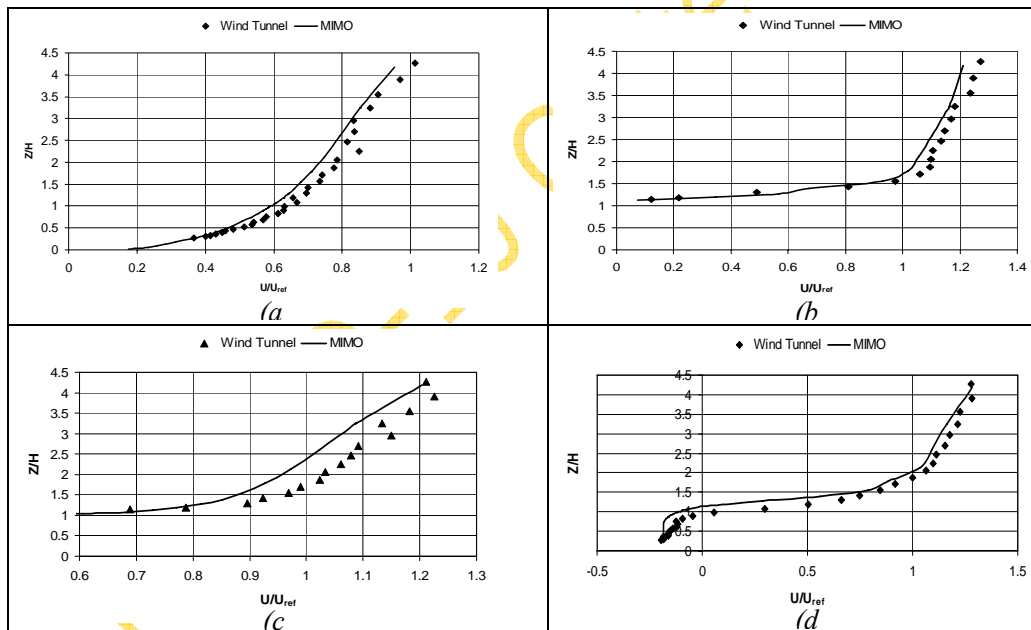


Fig. 4; Comparison between numerical results and wind tunnel measurements of the normalized u - component at (a) upstream, (b) and (c) above the roof level and (d) downstream of the containers array.

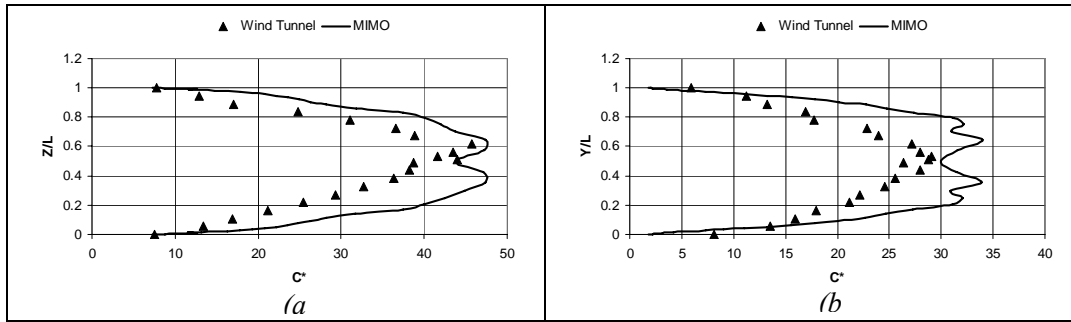


Fig. 5; Comparison between numerical results and wind tunnel measurements of in street dimensionless concentration near (a) the leeward and (b) the windward walls at a height of $Z=0.3H$.

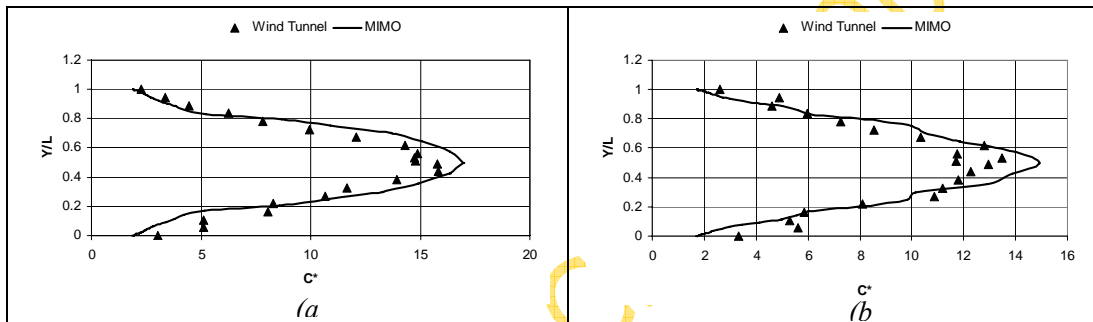


Fig. 6; Comparison between numerical results and wind tunnel measurements of in-street dimensionless concentration near (a) the leeward and (b) the windward walls at a height of $Z=0.5H$.

For the case of the wind approaching at an angle of 12° however, mass transport is strongly influenced by the lateral velocity component, since a considerable amount of mass is transported to one side of the street canyon with a corresponding reduction of the mass leaving the street canyon via the roof top.

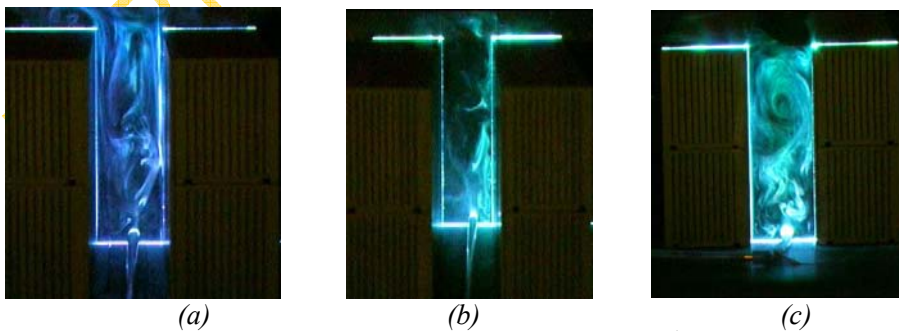


Fig. 7; Flow visualisation images of vertical planes inside the 2nd consecutive street canyon: (a) centre, (b) right side edge and (c) left side edge.

Additionally, the visualisation experiments that were carried out for five different approach flow wind directions (Figures 7a-7c), revealed that the ventilation mechanism of the street canyon is very sensitive to the direction of the approach flow. Already small deviations from perpendicular, lead to a significant street-parallel velocity component with a corresponding transport of pollutants to the canyon edge.

CONCLUSIONS

Overall, comparison between numerical results and re-scaled wind tunnel measurements shows good agreement between the two. However, numerical results indicate that the predicted velocity field has been slightly underestimated by MIMO and as a result the corresponding concentration has been, also slightly, overestimated.

Further in conclusion, for the case of the wind direction being perpendicular to the street canyon axis, the concentration measurements that were carried out demonstrated that the pollution inside the street canyon is accumulated in the middle of the street canyon, with the highest concentrations, as expected (*Sini et al. 1996*), at the lowest levels. Moreover, the visualisation experiments for this case showed that pollutants are flushed out mainly via the roof top, with only a small portion leaving the canyon at the sides. However, when the wind is approaching at (even small) angles with respect to the street canyon axis, the flushing via one canyon side is considerably enforced with a corresponding reduction of the mass transported out of the street canyon via the roof top.

ACKNOWLEDGEMENTS

The authors gratefully acknowledge funding from the EU ATREUS project (HPTN-CT-2002-002079).

REFERENCES

- [1] Barmpas, P., B. Leidl, N., Moussiopoulos and M., Schatzmann, 2005: Physical modeling of flow and dispersion in and around an idealized street canyon – replicating the PICADA field experiment in a boundary layer wind tunnel. Proceedings of the 5th International Conference on Urban Air Quality, Valencia, Spain 29-31 March.
- [2] Ehrhard, J., I.A. Khatib, C. Winkler, R. Kunz, N. Moussiopoulos and, G. Ernst, 2000: The microscale model MIMO: development and assessment. Journal of Wind Engineering and Industrial Aerodynamics, **85**, 163-176.
- [3] Kunz, R., 2001: Mathematische Modellierung des atmosphärischen Stofftransports und des Mikroklimas in bebauten Gebieten, VDI Verlag, Reihe 15, Nr. 236.
- [4] Moussiopoulos, N., I., Ossanlis, P., Barmpas and J., Bartzis, 2005: Comparison of numerical and experimental results for the evaluation of the depollution effectiveness of photocatalytic coverings in street canyons. Proceedings of the 5th International Conference on Urban Air Quality, Valencia, Spain 29-31 March.
- [5] Schatzmann, M. and Leidl, B., 2002: Validation and application of obstacle-resolving dispersion models. Atmospheric Environment, 36, 4811– 4821.
- [6] Sini, J.F., S. Anquetin and P.G. Mestayer, 1996: Pollutant dispersion and thermal effects in urban street canyons. Atmospheric Environment, **30**, 2659-2677.
- [7] VDI 3738 Part 12: Environmental meteorology, Physical modeling of flow and dispersion processes in the atmospheric boundary layer, Application of wind tunnels.